Biophysical Journal Volume 109 July 2015 330–339

Article

DMSO Induces Dehydration near Lipid Membrane Surfaces

Chi-Yuan Cheng,[1] Jinsuk Song,[1] Jolien Pas,[2] Lenny H. H. Meijer,[2] and Songi Han[1,*]

[1]Department of Chemistry and Biochemistry, University of California, Santa Barbara, Santa Barbara, California; and [2]Department of Biomedical Engineering, Laboratory of Chemical Biology and Institute for Complex Molecular Systems, Eindhoven University of Technology, Eindhoven, the Netherlands

ABSTRACT Dimethyl sulfoxide (DMSO) has been broadly used in biology as a cosolvent, a cryoprotectant, and an enhancer of membrane permeability, leading to the general assumption that DMSO-induced structural changes in cell membranes and their hydration water play important functional roles. Although the effects of DMSO on the membrane structure and the headgroup dehydration have been extensively studied, the mechanism by which DMSO invokes its effect on lipid membranes and the direct role of water in this process are unresolved. By directly probing the translational water diffusivity near unconfined lipid vesicle surfaces, the lipid headgroup mobility, and the repeat distances in multilamellar vesicles, we found that DMSO exclusively weakens the surface water network near the lipid membrane at a bulk DMSO mole fraction (X_{DMSO}) of <0.1, regardless of the lipid composition and the lipid phase. Specifically, DMSO was found to effectively destabilize the hydration water structure at the lipid membrane surface at X_{DMSO} <0.1, lower the energetic barrier to dehydrate this surface water, whose displacement otherwise requires a higher activation energy, consequently yielding compressed interbilayer distances in multilamellar vesicles at equilibrium with unaltered bilayer thicknesses. At X_{DMSO} >0.1, DMSO enters the lipid interface and restricts the lipid headgroup motion. We postulate that DMSO acts as an efficient cryoprotectant even at low concentrations by exclusively disrupting the water network near the lipid membrane surface, weakening the cohesion between water and adhesion of water to the lipid headgroups, and so mitigating the stress induced by the volume change of water during freeze-thaw.

INTRODUCTION

Dimethyl sulfoxide (DMSO) has been broadly used for a long time in biology for diverse applications (1). For example, it works as an efficient cryoprotectant that prevents cellular damage during freeze-thaw at relatively low concentrations (<10 mol %) (2–5). DMSO at higher concentrations (>60 mol %) enhances cell membrane permeability as a transdermal permeation enhancer in cosmetics (6), as well as in drug delivery applications (7). Despite the extensive use of DMSO in a broad range of biological applications, its formulation is tuned purely empirically and the basis of its diverse effects on biological membranes is unclear. To understand the mechanism behind the biological function of DMSO for its optimal and rational implementation, it is essential to know how DMSO influences the lipid membrane structure, as well as the hydration water structure and dynamics at the membrane-water interface.

In DMSO/water binary solutions, the DMSO oxygen can form strong hydrogen bonds with the water hydrogens. A microwave dielectric relaxation spectroscopy study reported that the dielectric relaxation time is maximal at a DMSO mole fraction in a DMSO/water mixture, X_{DMSO}, of 0.33, suggesting a stoichiometric composition of H_2O-DMSO-H_2O (8). Moreover, the free energy of activation for the dielectric relaxation process is increased by ~5 kJ/mol at $X_{DMSO} = 0.33$, compared with that in pure water (8). Additionally, the self-diffusion coefficients of DMSO and H_2O are both found to be slowest between $X_{DMSO} = 0.3$ and 0.4 (9). Although the detailed structure and precise nature of the DMSO-water hydrogen bonds are not fully understood, it is clear that direct DMSO-water interaction is strongest at a DMSO/H_2O molar ratio of 1:2 (10,11).

DMSO at concentrations up to $X_{DMSO} = 0.3$ has been shown to increase the surface tension of 1,2-dipalmitoyl-*sn*-glycero-3-phosphocholine (DPPC) monolayers at the air-water interface (12) and to weaken the sharp liquid expanded-to-liquid condensed phase transition by enhancing the alkyl chain ordering even at low surface lipid coverage (13–15). The influence of DMSO on fully hydrated lipid bilayer structures is even more dramatic. In the most frequently studied DPPC vesicle membranes, several small angle x-ray scattering (SAXS) and small angle neutron scattering studies revealed that the multilamellar repeat distance decreases sharply with increasing DMSO concentration up to $X_{DMSO} = 0.13$, although the thickness of the DPPC bilayer remains unchanged up to $X_{DMSO} = 0.3$ (16–19). Not surprisingly, DMSO exerts similar effects on the 1,2-dimyristoyl-*sn*-glycero-3-phosphocholine bilayers in the fluid phase of decreasing the interstitial water layers, although not affecting the bilayer thickness up to $X_{DMSO} = 0.4$ (20), as well as decreasing the repeat spacing for both the lamellar and the hexagonal

Submitted April 21, 2015, and accepted for publication June 9, 2015.

*Correspondence: songi@chem.ucsb.edu

Editor: Francesca Marassi.

0006-3495/15/07/0330/10 $2.00

http://dx.doi.org/10.1016/j.bpj.2015.06.011

phases of 1,2-dipalmitoleoyl-*sn*-glycero-3-phosphatidylethanolamine membranes (21). It is agreed that the decrease in multilamellar repeat distance is a consequence of a reduction in the interbilayer interstitial water layer thickness, whose origin was attributed to dehydration driven by DMSO (16–19). DMSO has also been shown to generally increase the phase stability of phosphatidylcholine (PC) membranes (19,22). However, a mechanistic understanding and direct evidence supporting the role of water in these processes are missing.

The effect of DMSO on lipid bilayers has been studied extensively by molecular dynamics (MD) simulations, which were carried out at elevated temperatures (T >25°C) to ensure that the lipid membrane is in the fluid phase. Although there are qualitative agreements among MD studies in that DMSO can induce the bilayer thinning and pore formation (23–26), the quantitative DMSO concentration at which the specific changes of bilayer structures occur is model-dependent. Of importance, the qualitative change induced by DMSO according to MD simulation contradicts experimental results. At X_{DMSO} <0.1, MD simulations reported that DMSO increases the area per lipid and induces membrane thinning in the fluid phase (23–26) for both DPPC and 1,2-dioleoyl-*sn*-glycero-3-phosphocholine (DOPC) membranes. This finding is contrary to experimental results which unambiguously show that the bilayer thickness remains constant in DPPC (18) and 1,2-dimyristoyl-*sn*-glycero-3-phosphocholine (20), not only in the gel, but also in the fluid phase at elevated temperatures. MD simulations also suggest that increasing DMSO concentration causes pore formation in the lipid bilayer (23–26), which can be reconciled with experimental findings that higher DMSO concentration enhances the solvent permeability of the cell membrane (6). If the DMSO concentration is higher than needed for stable pore formation, the bilayer structure becomes unstable and disintegrates according to MD simulations (23,24). However, such membrane rupture has never been experimentally observed at high DMSO concentrations.

The challenge is that despite an extensive list of experimental and computational research reported on the phase behavior and structural changes of lipid self-assemblies induced by DMSO (16–26), there are no experimental studies on directly examining the DMSO-induced modulation of the hydration water structure and dynamics at the lipid membrane surface. In this work, we report on changes in the local translational diffusivity of water near lipid bilayer surfaces measured by Overhauser dynamic nuclear polarization (ODNP) relaxometry (27–30), as induced by the addition of DMSO at a low concentration of X_{DMSO} <0.1, although in contrast the lipid structure and lipid headgroup ordering remain unaffected by DMSO. Changes in the translational diffusivity of hydration water near the lipid bilayer surface, in the absence of confinement effects, offer direct experimental evidence for the effect of DMSO on the hydrogen bond breaking and reforming equilibrium, and so on the strength of the cohesive water network hydrating the lipid membrane headgroups. However, instead of DMSO replacing the hydration water of the lipid headgroups, which has been implied by several studies as a dehydration effect in the literature (16,17,26), our experimental results converge to a molecular model in which DMSO competes for the surface hydration water to weaken its attraction to lipid headgroups of large unilamellar vesicles (LUVs), as well as to weaken the cohesive hydration water network by preferential orientation of DMSO with its sulfoxide moiety facing away from the water solvent. Under these conditions, when lipid surfaces closely approach each other, as found in the interstitials of multilamellar vesicles (MLVs), the dehydration and expulsion of surface water in the weakened hydration layers is facilitated by DMSO, resulting in a decreasing equilibrium interstitial (interlamellar) distance.

MATERIALS AND METHODS

Materials

All lipids were obtained from Avanti Polar Lipids (Alabaster, AL) and used without further purification. Deuterated DMSO (DMSO-d6, 99.9%) was acquired from Cambridge Isotope Laboratories (Andover, MA). Cholorform and methanol used for dissolving the lipids were obtained from Fisher Scientific (Pittsburg, PA). In this study, the lipid constituents for the LUV and MLV membranes were DPPC or DPPC/dipalmitoyl phosphatidylglycerol (DPPG) (4:1 mol ratio) that are in the gel phase at 25°C, and DOPC or DPPC/1,2-dioleoyl-3-trimethylammonium-propane (DOTAP) (4:1 mol ratio) that are in the fluid phase at 25°C. The chemical structures of the lipids and spin-labeled probes used in this study are shown in Fig. S1 in the Supporting Material. DPPG has a net negatively charged headgroup from the phosphate moiety, whereas DOTAP has a net positively charged headgroup from the choline moiety. The headgroups of DPPC and DOPC are zwitterionic.

Preparation of lipid vesicle samples

The lipid stocks were prepared by dissolving dry lipids in chloroform/methanol (4:1, v:v) and mixed at the desired proportions. The solvent was then evaporated under a stream of nitrogen. The traces of organic solvent were removed by evacuating the samples under vacuum for 24 h. The dried lipids were then rehydrated in a DMSO/water solution, which contained various DMSO concentrations at a temperature >20°C of gel-fluid lipid phase transition temperature with gentle vortexing for 1 h. The MLV samples were prepared through five freeze-thaw cycles, which consisted of 10 min of vortexing at a temperature >20°C of gel-fluid transition temperature and 10 min on ice without vortexing. Half of the MLV suspension was used to prepare the LUV samples. The LUVs were prepared by the extrusion method using filters with 200 nm pore diameter (Avanti Polar Lipids) above the gel-fluid transition temperature. The samples were prepared 24 h before measurements. Deuterated dimethyl sulfoxide (d6-DMSO, 99.9%, Cambridge Isotope Laboratories) was used for all ^{1}H ODNP and electron paramagnetic resonance (EPR) measurements.

ODNP and EPR experiments

For the ODNP and EPR measurements, a phospholipid spin probe TEMPO-PC (Avanti Polar Lipids), of which nitroxide radical is attached on the

choline moiety, is used (Fig. S1). The concentration of spin probe and lipid is 670 μM and 32 mM, respectively. ^{1}H ODNP experiments were performed at a 0.35 T electromagnet, operating at 14.8 MHz ^{1}H Larmor frequency and at 9.8 GHz electron Larmor frequency. A 4 μL sample was loaded into a 0.6 mm I.D., 0.8 mm O.D. quartz capillary tube (Fiber Optic Center, New Bedford. MA) and both ends sealed with beeswax. The capillary was mounted onto a homebuilt NMR probe with a U-shaped radiofrequency NMR coil (27). The EPR signal was acquired by a Bruker X-band EMX EPR spectrometer (Billerica, MA) with a dielectric resonator (model: ER 4123D). During ODNP experiments, the center field of nitroxide hyperfine transition lines was pumped continuously by microwave irradiation at 9.8 GHz, while the ^{1}H NMR signal was recorded. T_1 relaxation measurements were carried out using an inversion-recovery pulse sequence operated by a Bruker Avance spectrometer in a 0.35 T superconductive magnet or electromagnet. A standard $\pi/2$ pulse length was ~4 μs, and the recycle delay was 15 s. All the experiments were performed at room temperature.

SAXS

50 mg lipid was mixed with 100 mg of a DMSO/water solution. The MLV sample was prepared based on freeze-thaw cycles described previously. 10 μL MLV sample was then loaded into quartz capillary tubes with a 1.5 mm O.D. and a 0.01 mm wall thickness (Hampton Research, Laguna Niguel, CA). The capillary was sealed with beeswax and was kept at a temperature >20°C of the gel-fluid lipid phase transition temperature for 1 h before measurements. SAXS measurements were performed using a custom built x-ray diffractometer with a XENOCS Genix microsource (wavelength: 1.54 Å (Sassenage, France)) and a Bruker HI-STAR multiwire area detector (31). The integrated diffraction data were plotted as a function of $q = (4\pi/\lambda)\sin\theta$, where λ is the wavelength of the beam (λ=1.54 Å), and θ is the Bragg angle. The SAXS data were collected at a rate of 0.1°/min at room temperature. The repeat distance d of the multilamellar vesicles was determined from the position of the diffraction peak, following $d = 2\pi/q$. All diffraction patterns were processed and corrected for background scattering and sample attenuation using FIT2D (32).

^{31}P NMR

LUV samples for ^{31}P NMR measurements were prepared as described previously. Briefly, LUV suspensions (200 nm diameter) with 32 mM lipid were used, but were hydrated with a solution containing 10 vt% D_2O at a given DMSO concentration to enable a ^{2}H frequency lock. The homogenized samples were deposited into a 5 mm NMR glass tube (Norell, Landisville, NJ). The NMR tube was sealed with a rubber plug and paraffin. It has been shown that the lipid lamellar phase was preserved and was randomly oriented with respect to the external magnetic field under the experimental condition and preparation (33). ^{31}P NMR spectra at 25°C were acquired at a frequency of 161.98 MHz equipped with a Varian Unity Inova 400 MHz spectrometer (Palo Alto, CA) and a 5 mm broadband probe. Phosphoric acid in D_2O was used as an external reference at 0 ppm. The spectra were recorded under continuous broadband proton decoupling using the following parameters: a spectral width of 36 kHz; a $\pi/2$ pulse width of 5 μs; an interpulse delay of 5 s; 2048 numbers of transient. Each ^{31}P NMR spectrum was applied to a polynomial baseline correction, and was processed with 2 Hz line broadening. The ^{31}P NMR spectral lineshape shown in Fig. S4 is contributed from a random spatial distribution of bilayers (34). ^{31}P NMR spectra were analyzed using MATLAB (The MathWorks, Natick, MA) and the matNMR package (35).

RESULTS

The local translational diffusion coefficient of water within 10 Å of the lipid membrane surface, as denoted by $D_{surface}$, was measured by ODNP at various DMSO concentrations at 25°C (27). The detailed ODNP method and data analysis can be found in the Supporting Material. LUVs and MLVs made of the different types of lipids were investigated, to verify whether the effect of DMSO on the water diffusion at lipid membrane surfaces is a general effect, independent of lipid composition, hydrocarbon ordering, headgroup charge, and headgroup orientation. A nitroxide spin probe tethered off the choline group and located 5 Å out from the phosphate group, as a part of the TEMPO-PC lipid (Fig. S1), was employed at 2.5 mol % of the total lipid to measure water diffusion within 10 Å of the spin probe at unconfined LUV surfaces, as well as at the MLV surfaces within the confined interbilayer interstitial water layer by ODNP (36–38). Control experiments with smaller TEMPO-PC partitioning down to 1 mol % were carried out to rule out adverse effects exerted by the probe itself. The same TEMPO-PC probe was used to monitor the lipid headgroup dynamics by continuous wave EPR spectroscopy.

Fig. 1 *a* presents the ratio of the $D_{surface}$ value at MLV surfaces made of DOPC and DPPC within 10 Å of the TEMPO-PC's tethered radical (see Tables S1 and S2) and the D_{bulk} value determined using free radicals dissolved in bulk DMSO/water solution devoid of the lipid membrane (see

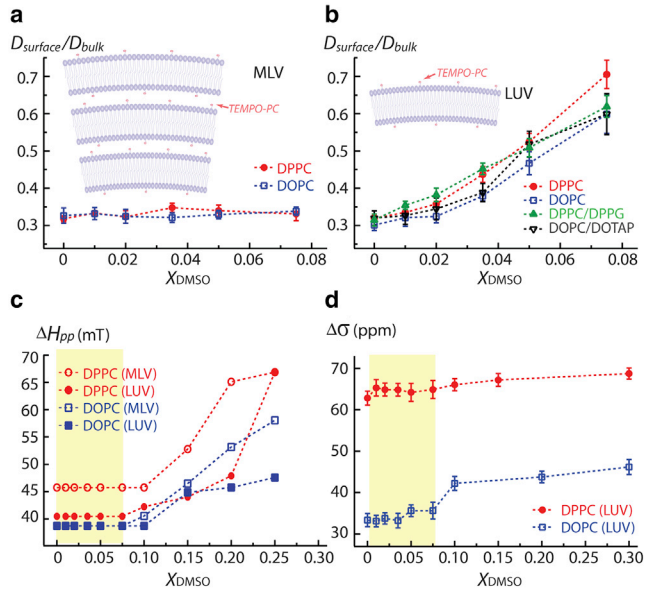

FIGURE 1 Ratio of water diffusion coefficient $D_{surface}$ at membrane surface and bulk water diffusion coefficient D_{bulk} in MLVs (*a*) and LUVs (*b*) at various DMSO molar fraction (X_{DMSO}) at 25°C. (*c*) The changes in peak-to-peak linewidth ΔH_{pp} deducted from the EPR spectra of the TEMPO-PC attached on the surface of LUVs and MLVs at various X_{DMSO} at 25°C. ΔH_{pp} is inversely proportional to the rotational mobility of the nitroxide spin attached at the lipid choline. (*d*) ^{31}P CSA ($\Delta\sigma$) of the phosphate group at LUV surfaces at various X_{DMSO} at 25°C. Yellow areas in (*c*) and (*d*) are the region of low DMSO concentration where ODNP is performed and presented in (*a*) and (*b*). The error bar represents standard deviation of the parameter estimated from the fitting. To see this figure in color, go online.

Table S3), and that as a function of bulk DMSO concentration. Notably, the measurements of surface water diffusion are focused on the regime of X_{DMSO} <0.1, where DMSO does not influence the bilayer thickness (16–19) and lipid headgroup rotational motion, as will be discussed later in this section.

In the absence of DMSO, the $D_{surface}$ value at MLV surfaces made of DPPC and DOPC was found to be ~7.7 × 10^{-10} m^2/s, presenting an ~threefold retardation, compared to the bulk water diffusivity with $D_{bulk} = 2.3 \times 10^{-9}$ m^2/s (39). This retardation is expected as the lipid vesicle surface is hydrophilic and locally charged (even for zwitterionic PC), yielding stronger hydrogen bond networks between water molecules near the lipid headgroups than between water molecules in the bulk (36–38). When normalizing $D_{surface}$ at MLV surfaces in the presence of DMSO with D_{bulk} of the solution containing the same DMSO concentration, $D_{surface}/D_{bulk}$ is found to be constant for all MLVs at $0 \leq X_{DMSO} \leq 0.075$ (Fig. 1 *a*). As already mentioned, DMSO retards bulk water diffusion up to X_{DMSO} ~0.33 by forming stronger hydrogen bonds between DMSO and water (8–11). Consequently, water viscosity increases in bulk solution with increasing DMSO concentration, as verified by a decrease in D_{bulk} measured by ODNP using free nitroxide radicals in DMSO/water solutions (Table S3). Therefore, a constant $D_{surface}/D_{bulk}$ value in MLVs with increasing DMSO concentration suggests that the same retardation effect of DMSO on water dynamics in bulk solution is effective in the MLV interstitial, and thus that the DMSO concentration at the MLV surface within the interstitial is equal to that in bulk solution. Concurrently, the MLV interbilayer interstitial distance decreases with increasing DMSO concentration at equilibrium (16–19), implying that the physical confinement itself does not directly affect the water diffusivity in the MLV interstitial.

Fig. 1 *b* presents the $D_{surface}/D_{bulk}$ value at unconfined LUV surfaces as a function of bulk DMSO concentration. In the absence of DMSO, the $D_{surface}$ value at LUV surfaces made of DPPC, DOPC, DPPC/DPPG, and DOPC/DOTAP were around 7.2~7.7 × 10^{-10} m^2/s, similar to that at MLV surfaces in the interstitials. This result further verifies that the physical confinement within the MLV interstitials is not responsible for the retarded water diffusivity observed at the lipid membrane surface. In stark contrast to the constant value of $D_{surface}/D_{bulk}$ found at MLV surfaces with increasing DMSO concentrations, the trend for $D_{surface}/D_{bulk}$ exhibits a clear increase with increasing DMSO concentrations at LUV surfaces (see Tables S1–S3 for listed $D_{surface}$ and D_{bulk} values). These trends of enhanced $D_{surface}/D_{bulk}$ at LUV surfaces are upheld regardless of the lipid phase, composition, and headgroup charges. The observed increase in water diffusivity on LUV surfaces with increasing DMSO concentration relative to the bulk water diffusivity in DMSO/water solution implies that the local surface water experiences a lower viscosity that arises from a weakened solvent interaction within the surface hydration network compared to in bulk solution, in the complete absence of confinement effects at LUV surfaces. Gratifyingly, we observe the same trend of enhanced surface water diffusion in the presence of DMSO when DPPC (LUV) is synthesized under biologically relevant solution conditions, such as in phosphate buffered saline buffer, which contains 10 mM PO_4^{3-}, 137 mM NaCl, and 2.7 mM KCl, at pH 7.4 (data presented in Fig. S2). DMSO at $X_{DMSO} = 0.05$ enhances the $D_{surface}/D_{bulk}$ value derived from surface water diffusion of DPPC (LUV) from 0.31 to 0.57 in phosphate buffered saline buffer, which is similar to the increase from 0.32 to 0.53 seen in pure water (see Fig. 1 *b*). This verification is highly important, as it points to the robustness and generality of the DMSO effect on LUV surfaces, and thus is highly relevant to verifying its cryoprotecting function. Consequently, the displacement of this lower-viscosity water is energetically facilitated, whose effect however only results in the eviction of water when a compressive or attractive force is exerted to this hydration layer by a closely approaching surface, as found in MLVs. The molecular model and mechanism of this effect will be described in detail in the Discussion section.

To explicitly delineate the effects of DMSO on the ordering of lipid headgroups, the peak-to-peak central linewidth, ΔH_{pp}, of its first derivative EPR spectrum (Fig. S3) was used to deduce the rotational mobility of the nitroxide radical attached to the choline moiety of TEMPO-PC at various DMSO concentrations (40). Fig. 1 *c* shows the trends for the changes in the ΔH_{pp} value of TEMPO-PC's nitroxide probe near the lipid headgroups of MLVs and LUVs composed of DOPC and DPPC at various DMSO concentrations. The ΔH_{pp} values were found to be independent of the DMSO concentration at X_{DMSO} <0.1 for all samples studied here. Conversely, at X_{DMSO} >0.1, the ΔH_{pp} value gradually increases with increasing DMSO concentration, but not to the same extent in all lipid membrane samples. Additionally, we calculated the order parameters of surface spin probes incorporated into DOPC and DPPC liposomes and found results that are consistent with that presented in Fig. 1 *c*. The detailed analysis of the order parameters deducted from the EPR lineshape can be found in Fig. S6. In general, the nitroxide of TEMPO-PC as embedded in DPPC (gel phase) is more ordered than in DOPC (fluid phase) at X_{DMSO} >0.1 at room temperature. Overall, the analysis of ΔH_{pp} suggests that DMSO does not affect the mobility of the nitroxide/choline groups at X_{DMSO} <0.1.

To further examine the effect of DMSO on the structural ordering of lipid headgroups, the anisotropic motion of lipid phosphate in DOPC and DPPC (LUV) at various DMSO concentrations was quantified by the ^{31}P chemical shift anisotropy (CSA), $\Delta\sigma$ (Fig. 1 *d*), measured by the frequency separation of the low- and high-field shoulders of a static ^{31}P NMR spectrum (Fig. S4) at ambient temperature. The

characteristic ^{31}P CSA of lipid headgroups reflects on the restriction in averaging of the rotational motion around the P-O(glycerol) bond and the wobbling of the headgroup with respect to the bilayer normal (34,41,42). The trend of $\Delta\sigma$ in Fig. 1 *d* is consistent with that of the EPR ΔH_{pp} value (Fig. 1 *c*), both of which parameters suggest that DMSO does not alter the overall mobility of PC headgroups at X_{DMSO} <0.1. Notably, the $\Delta\sigma$ value found for DPPC is by 30 ppm larger than that for DOPC at 0 < X_{DMSO} <0.3, confirming that the anisotropic motion of the phosphate group is overall slower in the gel phase than in the fluid phase, as expected. Overall, the nitroxide and phosphate mobilities are both slower in DPPC than in DOPC, because the area per lipid of DPPC in the gel phase with 48 Å^2 is smaller than of DOPC in the fluid phase with 72 Å^2 (see Fig. 2 *b*) (43–46).

At X_{DMSO} >0.1, DMSO does begin to restrict the local mobility of the lipid phosphate groups according to the increasing $\Delta\sigma$ values (Fig. 1 *d*), similar to what was found for the nitroxide/choline mobility of lipid bilayers from the EPR peak linewidth (Fig. 1 *c*). Notably, the effect of DMSO on the DPPC headgroups at X_{DMSO} >0.1 is much smaller than on the DOPC headgroups, because the phosphate mobility of DPPC is more restricted to begin with. The important overall finding is that DMSO does not modulate the lipid headgroup mobility at X_{DMSO} <0.1, in stark contrast to DMSO's direct influence on surface water diffusion observed near LUV surfaces, allowing us to conclude that DMSO exclusively and directly affects the surface water at X_{DMSO} <0.1.

When turning to DMSO-induced consequences for MLVs, our SAXS data show that changes in the repeat distance in MLV occur mostly at the lower DMSO concentration of X_{DMSO} <0.1 for both DPPC and DOPC membranes (Fig. 2 *a*, *yellow area*), which is consistent with literature findings (Fig. S5) (16–18). As a control, D_2O was added at the same concentration as DMSO to the solution of DOPC vesicles, and it was verified that solvent deuteration does not affect the SAXS results (See Table S6).

To further understand the mechanism of DMSO affecting the surface hydration layer of lipid membranes, the effect of DMSO on the energetics of surface water diffusion is directly evaluated by measuring the change in activation energy for surface water diffusion. The activation energy of water diffusion (E_a) is the effective energy barrier for a water molecule to diffuse and exchange its physical positions, which therefore necessarily requires the breaking and reforming of hydrogen bonds of water with the lipid headgroups and with other water molecules. Thus, E_a reflects on the strength of the dynamic network of water hydrating the LUV surface, whereby both the adhesive interaction between PC headgroups and directly bound water and the cohesive interaction between water molecules near the surface affect E_a. The E_a value at LUV surface is obtained by measuring $D_{surface}$ as a function of temperature (T) using the Arrhenius relation (37): $E_a = -k_B\,\partial(lnD_{surface})/\partial(1/T)$, with the Boltzmann constant k_B. This activation energy reports on the enthalpic contribution of hydration as diffusion of water does not involve changes in the entropy of the system, so that it is not clear how large the entropic contribution is to the binding free energy of water to the lipid surface. Fig. 3 shows the Arrhenius plot and the activation energy of water diffusion at DPPC LUV surfaces at X_{DMSO} = 0.05 and in the absence of DMSO. E_a of 28.7 kJ/mol at the DPPC LUV surface in the absence of DMSO is substantially lowered to 21.6 kJ/mol with X_{DMSO} = 0.05, implying that DMSO weakens the interactions between water molecules and their local environment near LUV surfaces. Specifically, the difference ΔE_a = 7.1 kJ/mol corresponds to 2.9 k_BT at 25°C, and thus is nonnegligible with respect to thermal energy. This finding corroborates the hypothesis that DMSO facilitates

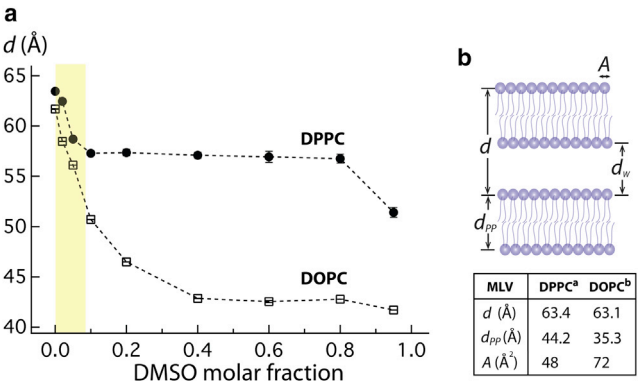

FIGURE 2 (*a*) DMSO concentration dependence of the repeat distance (*d*) of DPPC and DOPC MLVs measured by SAXS at 28°C. Yellow area is the DMSO concentration used in the ODNP experiment in Fig. 1, *a* and *b*. (*b*) Schematic diagram of MLV system. Repeat distance (*d*), bilayer thickness (d_{pp}), intermembrane distance (d_w), and surface area per lipid (*A*) are indicated in the figure. The literature values are cited from (43 and 44). To see this figure in color, go online.

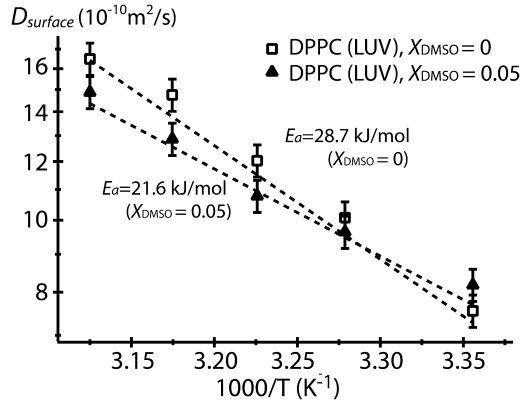

FIGURE 3 Activation energy (E_a) of water diffusion on the DPPC LUV surface in the presence and absence of DMSO. The dashed lines are a linear fit to the Arrhenius equation (E_a = 19.2 kJ/mol for bulk water).

the displacement of water. Taken together, the concurrent increase in the $D_{surface}/D_{bulk}$ value with a decrease in E_a for $D_{surface}$ at LUV surfaces in the presence of DMSO offers experimental evidence that DMSO actively weakens the dynamic hydrogen bond network. The dehydration in the sense of physical eviction or reduction of density of water at the LUV surface does not occur, because headgroups of LUV face an ocean of water. Crucially, the observation of an enhanced hydration dynamics at LUV surfaces by DMSO requires the physical presence and specific preferential orientation of DMSO at the LUV surfaces, because isotropic distribution of DMSO in bulk solution is known to decrease the solvent dynamics (8–11). Thus, DMSO must be perturbing the hydration water at LUV surfaces at a low DMSO concentration of X_{DMSO} <0.1 by competing with and winning over the PC headgroups that also attract hydration water, by orienting the sulfoxide group toward the PC headgroups and away from the bulk water solvent. The effect of the anisotropic DMSO orientation at LUV surfaces will be followed up in greater detail in the Discussion section.

In summary, because DMSO has been found to not change the membrane structure and headgroup mobility at X_{DMSO} <0.1, although its effect on the surface water diffusion was found to be significant regardless of the lipid phase and composition, it can be inferred that at low concentration (X_{DMSO} <0.1), DMSO directly influences the hydration water rather than the lipid membrane structure or lipid dynamics. This finding implies that the observed compression of the interbilayer interstitial of MLV is a result of DMSO-induced dehydration effects. Interestingly, we concluded earlier that the DMSO concentration in the equilibrated MLV interbilayer interstitial is equal as in bulk solution, implying that any preferred DMSO orientation at LUV surfaces responsible for the enhanced surface water dynamics is abolished at MLV surfaces, once the reduced equilibrium interbilayer interstitial distance is reached upon eviction of interfacial water.

DISCUSSION

Model for DMSO-induced dehydration at membrane surfaces at X_{DMSO} <0.1

At the membrane surface, the zwitterionic PC headgroup of lipids is known to be aligned or slanted nearly parallel to the surface, with the vector connecting the phosphorus (P) and nitrogen (N) suggested to be <30° from the bilayer plane, according to MD simulation (24) and ^{2}H NMR studies (47). The PC headgroup with the slanted P-N vector can align with each other by dipole-dipole attraction aligning neighboring moieties, with both the phosphate and choline moieties fully hydrated at the membrane surface.

According to neutron diffraction studies (48), the sulfur atom of DMSO is attracted to the negatively charged phosphate group, whereas the bulky methyl groups of DMSO reside in the pocket made of phosphorus and four oxygens, in a 30 mol % DMSO/water solution in 1,2-dipropionyl-*sn*-glycero-3-phosphocholine (C_3-PC) lipids. DMSO has also been reported to partially dehydrate the phosphate group of DPPC monolayers (13) by replacing the interaction between water hydrogen and phosphate oxygen with DMSO sulfur-phosphate oxygen interaction. It has also been observed experimentally that DMSO can replace water molecules near the lipid headgroups (13,48), as supported by the observation that the ratio of DMSO over water coordination number around the phosphate group is unaltered from the DMSO/water concentration ratio in bulk solution (48). This corroborates the validity of our earlier stated postulation that DMSO is assuming an anisotropic orientation with respect to the LUV surface. Specifically, DMSO may dynamically replace the hydration water of the phosphate group and orient itself toward the phosphate with two methyl groups pointing outward from the phosphorous, illustrated as option (1) in Fig. 4, which will serve as hydrophobic sites for approaching water molecules, in the sense that direct coordination between the methyl groups and water will not occur or be weak. In the absence of alternative opportunities for water to coordinate strongly with nearby moieties of these methyl groups or to compensate for the loss of direct hydrogen bonding opportunity otherwise, the presence of these methyl groups will weaken the hydrogen bonds in this region. The hydration water near the positively charged nitrogen of the choline moiety can also be dynamically replaced by DMSO, as facilitated by the attraction between the choline nitrogen and DMSO oxygen (48). Again, the two dangling methyl groups of DMSO act as hydrophobic sites, unable to directly coordinate with nearby water molecules, thus weaken the hydrogen bonds surrounding

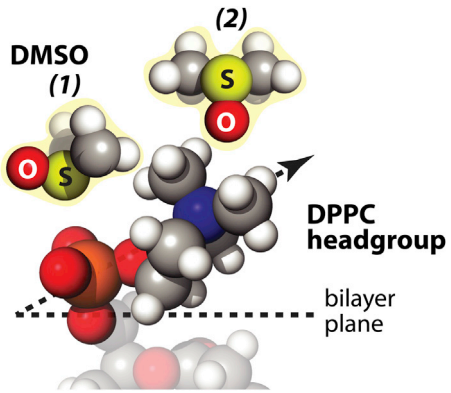

FIGURE 4 Schematic of hypothesized DMSO orientations at DPPC LUV surfaces that represent a snapshot of the most proximal configuration between DMSO and the lipid headgroups in a dynamic equilibrium, where DMSO does not permanently replace the bound hydration water of the PC headgroups. The DMSO's sulfur faces to lipid phosphate as represented (1), whereas the DMSO's oxygen is mainly taken up by the nitrogen atom of choline as represented (2). Water molecules are neglected in the figure for simplicity. To see this figure in color, go online.

the choline moiety, illustrated as option (2) in Fig. 4. When the DMSO oxygen is proximal to the choline group of the lipid headgroup, we propose that DMSO leaves no other strong hydrogen bonding sites available near choline, and thus exclude the chance of a balancing rehydration contribution at the lipid membrane surface. In contrast, when DMSO sulfur approaches the phosphate group of the lipid headgroup, DMSO oxygen should be left as a strong hydrogen acceptor, so that nearby water molecules can rehydrate DMSO oxygen. Our results, however, show that the dehydration effect dominates over the rehydration effect at the lipid membrane surface, as the $D_{surface}/D_{bulk}$ ratio increases with DMSO concentration (Tables S1–S3). Taken together, we postulate that DMSO prefers the orientation that exposes its methyl groups to bulk water, with two specific configurations shown as options (1) and (2) in Fig. 4, away from both the phosphate and choline moieties, thereby perturbing the surface water structure that would be otherwise hydrating the lipid headgroups. This specific orientation effect of DMSO at the lipid membrane surface of LUV and the resulting restricted motion of the lipid headgroups can be more effective at lipid membranes with smaller equilibrium area per lipid, such as DPPC compared to DOPC, as shown in Fig. 2 *b*. Taken together, our ODNP results imply that DMSO reduces the surface hydrophilicity, rather than increases the surface hydrophobicity of the LUV. It should be noted that the LUV surface is overall well hydrated and hydrophilic, and that there is no evidence that DMSO induces the formation of structured or more bound water on LUV surfaces. Although other scenarios, such as DMSO-DMSO interactions or nonideal hydrogen bonding geometries on the lipid membrane surface are possible that additionally can affect the DMSO-lipid headgroup interaction, it is necessary to emphasize that the two preferential orientations for DMSO as hypothesized in this study (Fig. 4) are the ensemble effect of many possible orientations of DMSO near the lipid membrane surface. Critically, DMSO is known to not strongly adsorb to PC headgroups (49). Thus, a dynamic equilibrium is expected with the configuration shown in Fig. 4 that presents a snapshot of one extreme configuration, where DMSO dynamically pulls at, but does not permanently replace, the bound hydration water of the PC headgroup.

As LUVs are dispersed homogeneously over the entire solution, the LUV can be approximated as a single membrane surface model. When two membrane surfaces approach closely as found in MLVs, they experience additional forces exerted by the neighboring lipid surface. The forces at MLV interlamellar spacing include attractive forces due to van der Waals and electrostatic forces, as well as repulsive forces due to the hydrated water and hydrated lipid headgroups (50). For zwitterionic DPPC and DOPC lipids, the electrostatic force is thought to be negligible compared with other forces. In any case, the interbilayer spacing in MLV is the space at which the attractive force, likely dominated by the van der Waals forces, matches the repulsive hydration or entropic forces of protruding lipid headgroups, at equilibrium. The question is whether DMSO reduces this equilibrium interbilayer distance by increasing the attractive force or decreasing the repulsive force. DMSO, however, is known to reduce the van der Waals attraction between membrane surfaces. Specifically, the Hamaker constant of the van der Waal force expression for the DMSO/water solution decreases by 30% when the dielectric spectral contribution of the solution medium is taken into account with increasing X_{DMSO} from 0 to 0.075 (50–52). Thus, if the reduction in the van der Waals force was the only contributing factor, the repeat distance between MLV surfaces should increase. At the same time, we know that the lipid headgroup dynamics and structure remain unaffected at X_{DMSO} <0.1, excluding their effect as a dominant factor. Apparently, DMSO reduces the repulsive hydration force more than it reduces the van der Waals force, resulting in the net effect of a decreasing repeat distance in MLVs with increasing DMSO concentration (16–18). By measuring an enhanced $D_{surface}/D_{bulk}$ and lowered E_a near unconfined LUV surfaces at X_{DMSO} <0.1, where LUV can be considered as a case with infinite interbilayer distances, this study offers direct and unprecedented experimental evidence that DMSO is weakening the dynamic network of water near the PC headgroups of LUV by DMSO, rather than simply evicting individual water molecules hydrating the lipid headgroups. Consequently, DMSO at this low concentration exclusively reduces the repulsive hydration forces at lipid membrane surfaces, evicts interstitial water between MLV surfaces in the course of equilibrating at a reduced interstitial water layer thickness (d_w) in the MLV (Fig. 2 *b*), where the anisotropic orientation of DMSO at the lipid headgroups of MLV is abolished once equilibrium is achieved. In other words, the reduced interstitial water layer thickness in MLVs is the result of DMSO-induced surface water dehydration, so that at equilibrium the DMSO-water distribution, concentration, and property as in bulk solution is restored in the interstitial layer of MLVs.

Effect of DMSO on the membrane structure and its biological function

At X_{DMSO} <0.1, DMSO is not penetrating into the hydrocarbon region (19), but it increases the gel-to-fluid phase transition temperature to stabilize the gel phase (18). Our study suggests that the increase in the gel-to-fluid phase transition temperature at X_{DMSO} <0.1 can only be mediated by the changes in the dynamic structure of surface hydration water near the lipid membrane, because neither the membrane thickness (16–18) nor the lipid headgroup mobility is affected. Notably, DMSO is often used as an efficient cryoprotectant precisely at this lower concentration regime (2–5). Although the role of DMSO as a cryoprotectant is

unclear, it was generally thought that the DMSO lowers the freezing point of water and causes water to form an amorphous glass state (1,2). In this study, we experimentally and directly verify the dehydration effect of DMSO, as a result of disrupting the dynamic hydrogen-bond water near the lipid membrane surface. We postulate that this perturbation of the surface hydration water network encompasses more than just the directly bound water to the lipid headgroups, and so can effectively mitigate freezing damages caused by the volume change between ice and liquid water, when the cell membrane solution is frozen in the presence of DMSO.

At $X_{DMSO} > 0.1$, the mobility of the lipid choline and phosphate headgroup starts to become restricted (Fig. 1, *c* and *d*). This effect occurs not only in MLVs but also LUVs, so that it is not originated from the approaching lipid membrane surfaces, but from DMSO itself. This lipid headgroup rigidification may come from DMSO-induced lateral attraction between lipids, as was observed in DPPC monolayers at the air-water interface (13). The lipid headgroup motion is constrained either by the lateral attraction between lipids induced by DMSO or by the intercalated DMSO between the lipid headgroups.

It is clear that the physicochemical effect of DMSO on lipid membrane surfaces is complex and significant at a broad range of DMSO concentration, whereas the molecular mechanism of DMSO's functional effect at higher concentration of $X_{DMSO} > 0.3$ on lipid membranes is yet to be systematically studied. Our study shows that DMSO not only clearly affects the lipid membrane, but also directly modulates the hydration water at the lipid membrane surfaces, whose effect and role must be considered in a unified picture on the molecular and thermodynamic basis of DMSO's effect on biological lipid membranes.

CONCLUSIONS

Effects of DMSO on lipid membranes and their hydration water were studied experimentally by ODNP, EPR, ^{31}P NMR, and SAXS methods. At a low DMSO concentration of $X_{DMSO} < 0.1$, surface-specific orientation of the sulfoxide group of DMSO causes water bound to the lipid headgroups of LUV to be pulled away and/or dynamically replaced by DMSO, without affecting the lipid headgroup dynamics and structure. More importantly, DMSO's preferred orientation at the LUV surfaces results in the two DMSO methyl groups facing the water solvent phase and perturbs a broader population of water that span a network of water hydrating the lipid headgroup, which includes water beyond the individual water molecules hydrogen bond to phosphate or choline moieties. The weakening of a hydrogen bond network of water observed near LUV surfaces by DMSO is in stark contrast to the known effect of DMSO of fortifying the hydrogen bonds with water in bulk solution. We observe this effect on the surface of both liquid-crystalline and gel phase LUVs, although a stronger effect is observed with gel phase LUVs. This effect of DMSO as manifested in enhanced surface water diffusivity and lowered diffusion activation energy at LUV surfaces is no longer observable at MLV surfaces, once equilibrium is reached at a reduced MLV interbilayer distance and after the fragile surface waters are expelled, where the physical property of bulk DMSO/water solution is restored in the interstitial. It should be noted that it is challenging to directly measure DMSO orientation on the LUV surface—in fact, we cannot think of an adequate experimental approach that is applicable to LUV surfaces under dilute solution conditions. Thus, we provide a hypothesized molecular model in Fig. 4, as derived from our experimental observation, that can be tested in the future to provide a molecular understanding of DMSO's effect at LUV surfaces. We suggest DMSO prevents freeze damage of the cell membrane by perturbing the water network hydrating the immediate cell surface to minimize water volume change between ice and liquid water that otherwise cannot easily yield to structural changes and cell death during freeze-thaw.

SUPPORTING MATERIAL

Supporting Materials and Methods, six figures, and six tables are available at http://www.biophysj.org/biophysj/supplemental/S0006-3495(15)00593-7.

AUTHOR CONTRIBUTIONS

C.-Y.C., J.S., and S.H. designed research; C.-Y.C., J.S., J.P., and L.H.H.M. performed research; C.-Y.C., J.S., J.P., L.H.H.M., and S.H. contributed new reagents/analytic tools; C.-Y.C., J.S., and S.H. analyzed data; and C.-Y.C., J.S., and S.H. wrote the article.

ACKNOWLEDGMENTS

We thank Alex Schrader, Steven Donaldson, and Prof. Jacob Israelachvili for critical and fruitful discussion.

This work was supported by the 2011 National Institutes of Health (NIH) Directors New Innovator Award and the Cluster of Excellence RESOLV (EXC 1069) funded by the Deutsche Forschungsgemeinschaft. This study made use of the Materials Research Laboratory (MRL) Central Facilities supported by the National Science Foundation (NSF) through the Materials Research Science and Engineering Centers under grant No. DMR 1121053. The MRL is a member of the NSF-funded Materials Research Facilities Network (www.mrfn.org). This work was also supported by UCSB-Cooperative International Science and Engineering Internship (CISEI) through the NSF Research Experiences for Undergraduates (NSF DMR 0843934) and the Eindhoven University of Technology to J.P. and L.H.H.M.

REFERENCES

1. Yu, Z. W., and P. J. Quinn. 1994. Dimethyl sulphoxide: a review of its applications in cell biology. *Biosci. Rep.* 14:259–281.

2. Anchordoguy, T. J., C. A. Cecchini, …, L. M. Crowe. 1991. Insights into the cryoprotective mechanism of dimethyl sulfoxide for phospholipid bilayers. *Cryobiology.* 28:467–473.
3. Rall, W. F., and G. M. Fahy. 1985. Ice-free cryopreservation of mouse embryos at -196 degrees C by vitrification. *Nature.* 313:573–575.
4. Lovelock, J. E., and M. W. H. Bishop. 1959. Prevention of freezing damage to living cells by dimethyl sulphoxide. *Nature.* 183:1394–1395.
5. Kasai, M. 2002. Advances in the cryopreservation of mammalian oocytes and embryos: development of ultrarapid vitrification. *Reprod. Med. Biol.* 1:1–9.
6. Williams, A. C., and B. W. Barry. 2004. Penetration enhancers. *Adv. Drug Deliv. Rev.* 56:603–618.
7. Barry, B. W. 2004. Breaching the skin's barrier to drugs. *Nat. Biotechnol.* 22:165–167.
8. Lu, Z., E. Manias, …, M. Lanagan. 2009. Dielectric relaxation in dimethyl sulfoxide/water mixtures studied by microwave dielectric relaxation spectroscopy. *J. Phys. Chem. A.* 113:12207–12214.
9. Packer, K. J., and D. J. Tomlins. 1971. Nuclear spin relaxation and self-diffusion in the binary system, dimethylsulphoxide (DMSO)+. *Trans. Faraday Soc.* 67:1302–1314.
10. Wong, D. B., K. P. Sokolowsky, …, M. D. Fayer. 2012. Water dynamics in water/DMSO binary mixtures. *J. Phys. Chem. B.* 116:5479–5490.
11. Schichman, S. A., and R. L. Amey. 1971. Viscosity and local liquid structure in dimethyl sulfoxide-water mixtures. *J. Phys. Chem.* 75:98–102.
12. Krasteva, N., D. Vollhardt, …, H. Mohwald. 2001. Effect of sugars and dimethyl sulfoxide on the structure and phase behavior of DPPC monolayers. *Langmuir.* 17:1209–1214.
13. Chen, X., and H. C. Allen. 2009. Interactions of dimethylsulfoxide with a dipalmitoylphosphatidylcholine monolayer studied by vibrational sum frequency generation. *J. Phys. Chem. A.* 113:12655–12662.
14. Jubb, A. M., W. Hua, and H. C. Allen. 2012. Organization of water and atmospherically relevant ions and solutes: vibrational sum frequency spectroscopy at the vapor/liquid and liquid/solid interfaces. *Acc. Chem. Res.* 45:110–119.
15. Chen, X., Z. Huang, …, H. C. Allen. 2010. Reorganization and caging of DPPC, DPPE, DPPG, and DPPS monolayers caused by dimethylsulfoxide observed using Brewster angle microscopy. *Langmuir.* 26:18902–18908.
16. Kiselev, M. A., P. Lesieur, …, M. Ollivon. 1999. DMSO-induced dehydration of DPPC membranes studied by X-ray diffraction, small-angle neutron scattering, and calorimetry. *J. Alloys Compd.* 286:195–202.
17. Gordeliy, V. I., M. A. Kiselev, …, J. Teixeira. 1998. Lipid membrane structure and interactions in dimethyl sulfoxide/water mixtures. *Biophys. J.* 75:2343–2351.
18. Tristram-Nagle, S., T. Moore, …, J. F. Nagle. 1998. DMSO produces a new subgel phase in DPPC: DSC and X-ray diffraction study. *Biochim. Biophys. Acta.* 1369:19–33.
19. Yu, Z. W., and P. J. Quinn. 1995. Phase stability of phosphatidylcholines in dimethylsulfoxide solutions. *Biophys. J.* 69:1456–1463.
20. Gorshkova, J. E., and V. I. Gordeliy. 2007. Investigation of nteraction of dimethyl sulfoxide with lipid membranes by small-angle neutron scattering. *Crystallography reports.* 52:535–539.
21. Kinoshita, K., S. J. Li, and M. Yamazaki. 2001. The mechanism of the stabilization of the hexagonal II (HII) phase in phosphatidylethanolamine membranes in the presence of low concentrations of dimethyl sulfoxide. *Eur. Biophys. J.* 30:207–220.
22. Chang, H. H., and P. K. Dea. 2001. Insights into the dynamics of DMSO in phosphatidylcholine bilayers. *Biophys. Chem.* 94:33–40.
23. Gurtovenko, A. A., and J. Anwar. 2007. Modulating the structure and properties of cell membranes: the molecular mechanism of action of dimethyl sulfoxide. *J. Phys. Chem. B.* 111:10453–10460.
24. Hughes, Z. E., A. E. Mark, and R. L. Mancera. 2012. Molecular dynamics simulations of the interactions of DMSO with DPPC and DOPC phospholipid membranes. *J. Phys. Chem. B.* 116:11911–11923.
25. Notman, R., M. Noro, …, J. Anwar. 2006. Molecular basis for dimethylsulfoxide (DMSO) action on lipid membranes. *J. Am. Chem. Soc.* 128:13982–13983.
26. Sum, A. K., and J. J. de Pablo. 2003. Molecular simulation study on the influence of dimethylsulfoxide on the structure of phospholipid bilayers. *Biophys. J.* 85:3636–3645.
27. Franck, J. M., A. Pavlova, …, S. Han. 2013. Quantitative cw Overhauser effect dynamic nuclear polarization for the analysis of local water dynamics. *Prog. Nucl. Magn. Reson. Spectrosc.* 74:33–56.
28. Hausser, K. H., and D. Stehlik. 1968. Dynamic nuclear polarization in liquids. *Adv. Magn. Reson.* 3:79–139.
29. Armstrong, B. D., and S. Han. 2009. Overhauser dynamic nuclear polarization to study local water dynamics. *J. Am. Chem. Soc.* 131:4641–4647.
30. Armstrong, B. D., and S. Han. 2007. A new model for Overhauser enhanced nuclear magnetic resonance using nitroxide radicals. *J. Chem. Phys.* 127:104508.
31. Li, Y. L., R. Beck, …, M. Divinagracia. 2008. Scatterless hybrid metal-single-crystal slit for small-angle X-ray scattering and high-resolution X-ray diffraction. *J. Appl. Cryst.* 41:1134–1139.
32. Facility, E. S. R. http://www.esrf.eu/computing/scientific/FIT2D/.
33. Cullis, P. R., and B. de Kruijff. 1979. Lipid polymorphism and the functional roles of lipids in biological membranes. *Biochim. Biophys. Acta.* 559:399–420.
34. Seelig, J. 1978. 31P nuclear magnetic resonance and the head group structure of phospholipids in membranes. *Biochim. Biophys. Acta.* 515:105–140.
35. van Beek, J. D. 2007. matNMR: a flexible toolbox for processing, analyzing and visualizing magnetic resonance data in MATLAB. *J. Magn. Reson.* 187:19–26.
36. Cheng, C. Y., J. Y. Wang, …, S. Han. 2012. An ultrasensitive tool exploiting hydration dynamics to decipher weak lipid membrane-polymer interactions. *J. Magn. Reson.* 215:115–119.
37. Kausik, R., and S. Han. 2009. Ultrasensitive detection of interfacial water diffusion on lipid vesicle surfaces at molecular length scales. *J. Am. Chem. Soc.* 131:18254–18256.
38. Song, J., J. Franck, …, S. Han. 2014. Specific ions modulate diffusion dynamics of hydration water on lipid membrane surfaces. *J. Am. Chem. Soc.* 136:2642–2649.
39. Stejskal, E. O., and J. E. Tanner. 1965. Spin diffusion measurements: spin echoes in the presence of a time-dependent field gradient. *J. Chem. Phys.* 42:288–292.
40. Columbus, L., and W. L. Hubbell. 2002. A new spin on protein dynamics. *Trends Biochem. Sci.* 27:288–295.
41. Dufourc, E. J., C. Mayer, …, G. Kothe. 1992. Dynamics of phosphate head groups in biomembranes. Comprehensive analysis using phosphorus-31 nuclear magnetic resonance lineshape and relaxation time measurements. *Biophys. J.* 61:42–57.
42. Kohler, S. J., and M. P. Klein. 1977. Orientation and dynamics of phospholipid head groups in bilayers and membranes determined from 31P nuclear magnetic resonance chemical shielding tensors. *Biochemistry.* 16:519–526.
43. Nagle, J. F., R. Zhang, …, R. M. Suter. 1996. X-ray structure determination of fully hydrated L alpha phase dipalmitoylphosphatidylcholine bilayers. *Biophys. J.* 70:1419–1431.
44. Tristram-Nagle, S., H. I. Petrache, and J. F. Nagle. 1998. Structure and interactions of fully hydrated dioleoylphosphatidylcholine bilayers. *Biophys. J.* 75:917–925.
45. Mills, T. T., G. E. S. Toombes, …, J. F. Nagle. 2008. Order parameters and areas in fluid-phase oriented lipid membranes using wide angle X-ray scattering. *Biophys. J.* 95:669–681.

46. Sun, W., R. M. Suter, …, J. F. Nagle. 1994. Order and disorder in fully hydrated unoriented bilayers of gel-phase dipalmitoylphosphatidylcholine. *Phys. Rev. E Stat. Phys. Plasmas Fluids Relat. Interdiscip. Topics.* 49:4665–4676.

47. Seelig, J., P. M. Macdonald, and P. G. Scherer. 1987. Phospholipid head groups as sensors of electric charge in membranes. *Biochemistry.* 26:7535–7541.

48. Dabkowska, A. P., F. Foglia, …, S. E. McLain. 2011. On the solvation structure of dimethylsulfoxide/water around the phosphatidylcholine head group in solution. *J. Chem. Phys.* 135:225105.

49. Kennedy, A., C. J. Long, …, T. J. Reid. 2003. The interaction of DMSO with model membranes. II. Direct evidence of DMSO binding to membranes: an NMR study. *J. Liposome Res.* 13:259–267.

50. Israelachvili, J. N. 1991. Intermolecular and Surface Forces. Academic, San Diego, CA.

51. Kaatze, U., R. Pottel, and M. Schafer. 1989. Dielectric spectrum of dimethyl suifoxide/water mixtures as a function of composition. *J. Phys. Chem.* 93:5623–5627.

52. LeBel, R. G., and D. A. I. Goring. 1962. Density, viscosity, refractive index, and hygroscopicity of mixtures of water and dimethyl sulfoxide. *J. Chem. Eng. Data.* 7:100–101.